Experimental verification of degrees of freedom for co-located antennas in wireless channels

Tian, Ruiyuan; Lau, Buon Kiong

Published in:
IEEE Transactions on Antennas and Propagation

DOI:
10.1109/TAP.2012.2196934

2012

Document Version:
Peer reviewed version (aka post-print)

Experimental Verification of Degrees of Freedom for Co-located Antennas in Wireless Channels

Ruiyuan Tian, *Student Member, IEEE,* and Buon Kiong Lau, *Senior Member, IEEE*

***Abstract*—It has been postulated that six co-located orthogonally polarized electrical and magnetic dipoles can offer up to six degrees of freedom (DOFs) in a multipath scattering environment. In other words, a six-fold increase in channel capacity can be achieved in the context of MIMO systems. However, due to the complexity in designing and measuring such a six-port antenna, to our knowledge, no experimental verification has yet been successfully performed. In this paper, the six DOFs hypothesis is experimentally verified at $377\,\mathrm{MHz}$. The experiment involves the design and fabrication of two six-port arrays. In particular, one array is made compact with co-located antenna elements enclosed in a small cubic volume of $(0.24\lambda)^3$. Using the two arrays, MIMO channel measurements are performed in a RF shielded laboratory in order to measure a multipath scattering environment. Analysis on eigenvalues of the measured channel shows that six DOFs are attained due to the orthogonality in radiation patterns of the two arrays.**

***Index Terms*—MIMO systems, polarization, antenna diversity.**

I. Introduction

MIMO systems employing multiple antenna elements at both the transmit (TX) and receive (RX) ends offer the potential to linearly increase capacity with an increase in the number of antennas [1]. Conventional MIMO systems make use of antenna arrays with spatially separated elements, and they perform best when the spatial correlation among the signals on different antenna branches is low, which typically requires the antenna elements to be separated by one half of a wavelength ($\lambda/2$). On the other hand, low signal correlation can also be obtained by utilizing polarization diversity [2]. The use of two polarization states of plane waves has been known to introduce two degrees of freedom (DOFs) in a wireless communication channel. However, an additional three-fold increase in channel capacity is shown in [3] by the use of six distinguishable electric and magnetic field components. Co-located, orthogonally polarized electric and magnetic dipoles are postulated to achieve six DOFs. Nevertheless, the experimental study in [3] demonstrates only three DOFs by means of tri-polarized half-wave sleeve dipoles, rather than the postulated six-fold capacity increase. This work has sparked further investigations on the number of DOFs that is theoretically available in wireless channels [4]–[7].

The analytical study in [8] shows that the array of co-located, orthogonally polarized, ideal electric and magnetic dipoles are capable of achieving the ultimate six communication modes in a channel model with uniform three-dimensional (3D) angular power spectrum (APS). Six DOFs are achieved by means of polarization and angle diversities obtained from the orthogonal radiation patterns of these electromagnetic energy density sensors [9]. Moreover, the study also suggests the use of half-wave dipoles and full-wave loops fails to attain this orthogonality. On the other hand, a MIMO cube antenna of 12 dipoles is proposed in [10]. For a very compact cube with side length of 0.05λ, six eigenchannels are theoretically obtained in a scattering environment with wide angular spreads at both the TX and RX ends. However, the first results are obtained by assuming no mutual coupling among the antennas. The further study in [11] reveals that mutual coupling causes significant degradations in the DOF performance of the cube, such that the side length of the cube needs to be at least 0.2λ in order to obtain six DOFs. This observation sheds some light on the impact of mutual coupling in realizing physically compact arrays that can effectively offer six DOFs.

Table I summarizes recent works on the practical design of compact antenna arrays with good DOF potential. To the best of the authors' knowledge, it remains challenging to design and measure a compact six-port antenna array that achieves six DOFs. In [21]–[23], conceptual six-port antenna prototypes are proposed analytically. Additionally, other multiport arrays with more practical antennas elements are also suggested. In [18], a six-port cube antenna of size $(0.43\lambda)^3$ is designed by combining tri-polarized PIFAs and slots. A six-port dielectric resonator antenna (DRA) array is reported in [19], where two compact DRA elements of size $0.16\lambda \times 0.16\lambda \times 0.12\lambda$ are

TABLE I
PRACTICAL ANTENNA ARRAY DESIGNS WITH GOOD DOF POTENTIAL.

Paper	Antenna Design
Stancil [12]	1-electric and 1-magnetic dipole
Skaufel [13]	1-electric dipole and 1-Alford loop [14]
Andrews [3]	tri-polarized sleeve dipoles
Chiu [15]	tri-polarized printed dipoles/slots
Gupta [16]	tri-polarized printed dipoles
Konanur [17]	tri-polarized dipoles + loop
Chiu [18]	6-port $(0.43\lambda)^3$-size cube (patches & slots)
Tian [19]	6-port $0.88\lambda \times 0.71\lambda \times 0.12\lambda$ DRA array
Chiu [20]	36-port $(1.13\lambda)^3$-size cube (slots)

Manuscript received June 22, 2011; revised November 14 and December 30, 2011. Current version published 20xx. This work was financially supported by VINNOVA (No. 2007-01377) and Vetenskapsrådet (No. 2006-3012).

R. Tian and B. K. Lau are with the Department of Electrical and Information Technology, Lund University, SE-221 00 Lund, Sweden. e-mail: {Ruiyuan.Tian, Buon_Kiong.Lau}@eit.lth.se.

Color versions of one or more of the figures in this paper are available online at http://ieeexplore.ieee.org.

Digital Object Identifier xx.xxxx/TAP.20xx.XXXXXXX

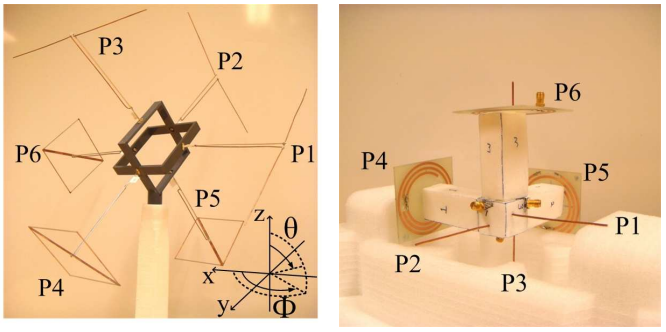

(a) Reference TX array (b) Compact RX array

Fig. 1. Six-port arrays. P1-P3/P4-P6 denote antenna ports for electric/magnetic dipoles of the TX and RX arrays.

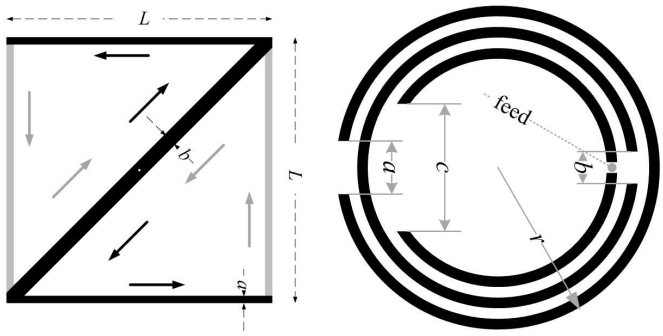

(a) Alford loop of TX array (b) SRR loop of RX array

Fig. 2. Design of the magnetic dipoles. (a) Alford loop: the dark and light areas denote the top and bottom copper layers of PCB, where the diagonal part is present on both layers with the feed in the center. The arrows illustrate the current flow formed by the two layers. (b) Planar SRR antenna.

placed on a larger ground plane with a separation distance of 0.44λ. Nevertheless, these arrays requires a certain spatial volume such that space, polarization and angle diversities are exploited simultaneously. No experiment has been performed successfully to verify the six DOFs hypothesis using the co-located arrays as proposed in [3].

In this paper, two six-port antenna arrays are designed and fabricated in order to investigate the number of DOFs in measured MIMO channels. In particular, the RX array is made compact in order to co-locate the antenna elements and to constrain the space diversity such that the obtained DOFs may be attributed to polarization and angle diversities. The TX array is significantly larger and designed for reference purpose. The antenna elements of both prototypes offer the desired characteristics of the fundamental electric and magnetic dipoles. In order to simplify the construction of the multiport array structures, as well as to utilize our MIMO channel sounding equipment, a relatively low operation frequency of $377\,\mathrm{MHz}$ is considered. Section II presents the arrays' design and characteristics. In Section III, 6×6 MIMO channel measurements using the two fabricated arrays are described. Analysis on eigenvalues of the measured channel matrices is performed in Section IV to investigate whether the compact six-port RX array can support six DOFs in the given setup. Section V concludes the paper.

II. Six-port Arrays

A. Reference TX Array

1) Array Design: The reference TX antenna array is designed by means of half-wave dipoles and Alford loops [14]. Figure 1(a) shows a picture of the prototype. In Fig. 2(a), the design principle of the Alford loop is illustrated. A double-sided PCB with a $1.55\,\mathrm{mm}$ thick FR4 substrate is used for printing the loop antenna. In order to reduce dielectric losses, we remove the parts of the substrate that have no copper strip on either side. Figure 2(a) also shows that the current is continuous along the circumference of the square loop formed by the two layers, whereas it is canceled on the diagonal part. In this way, the desired magnetic dipole characteristics are obtained. The resonant frequency is determined by the side length L, and the impedance matching of the antenna can be achieved by tuning the widths a and b. Design parameters as obtained from simulations in CST [24] are: $L = 145\,\mathrm{mm}$, $a = 2\,\mathrm{mm}$ and $b = 6\,\mathrm{mm}$, for the center frequency of $377\,\mathrm{MHz}$. Three Alford loops (Ports 4-6) are placed perpendicularly to one another as tri-polarized magnetic dipoles, which complement the three electric dipoles (Ports 1-3). Each of the six antennas is equipped with a quarter-wave balun to mitigate cable influence. The TX array can be enclosed in a cubic volume of $(0.75\lambda)^3$.

2) Array Characteristics: The measured scattering (S) parameters of the TX array are given in Fig. 3. The reflection coefficients show that the array bandwidth is limited by the loops to about $13.6\,\mathrm{MHz}$ at the $-6\,\mathrm{dB}$ level. Good isolation of more than $20\,\mathrm{dB}$ can be achieved between all pairs of antenna ports. In particular, the co-axial antenna pairs of electric and magnetic dipoles exhibit very low mutual couping around the resonant frequency, as can be observed from S_{41}, S_{52} and S_{63} in Fig. 3(b). The S parameters that are not shown exhibit similar behavior due to the symmetrical structure of the array. When measuring the TX array in a SATIMO Stargate 64 chamber [25], a coaxial cable is connected to the port being measured, with the other five ports terminated in $50\,\Omega$ loads. The average total efficiency is $88.4\%(-0.5\,\mathrm{dB})$ and $60.9\%(-2.1\,\mathrm{dB})$, for the electric and magnetic dipoles, respectively. Note that this antenna efficiency imbalance can lead to performance degradation as to be discussed in Section IV.

The measured gain patterns of the TX array for the ϕ- and θ-polarized components are illustrated in Figs. 4 and 5, respectively. The coordinate system of the measurement is given in Fig. 1(a). The patterns shown are normalized, such that the peak total gain is $0\,\mathrm{dB}$. It can be seen that, the patterns of the ϕ- and θ-polarized components interchange with each other between the electric and magnetic dipoles, from which good polarization diversity is attained. Additionally, angle diversity is also achieved since the antenna elements cover the whole sphere at distinct angular regions for a given polarization. One simple approach to characterize the DOF potential of a multiport array is to calculate the correlation between all pairs of antenna radiation patterns. At the center frequency, assuming an isotropic environment with uniform 3D APS, the correlation is found to be less than 0.13.

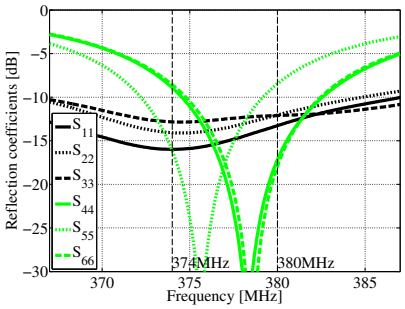

(a) Reflection coefficients: TX array

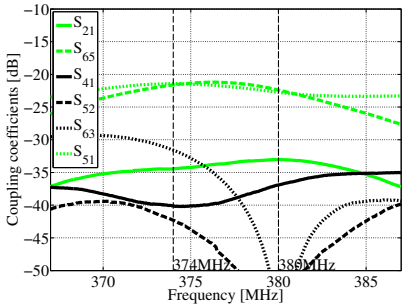

(b) Coupling coefficients: TX array

Fig. 3. Measured S parameters of the reference TX array. Ports 1-3 denote half-wave dipoles and Ports 4-6 denote Alford loops, respectively.

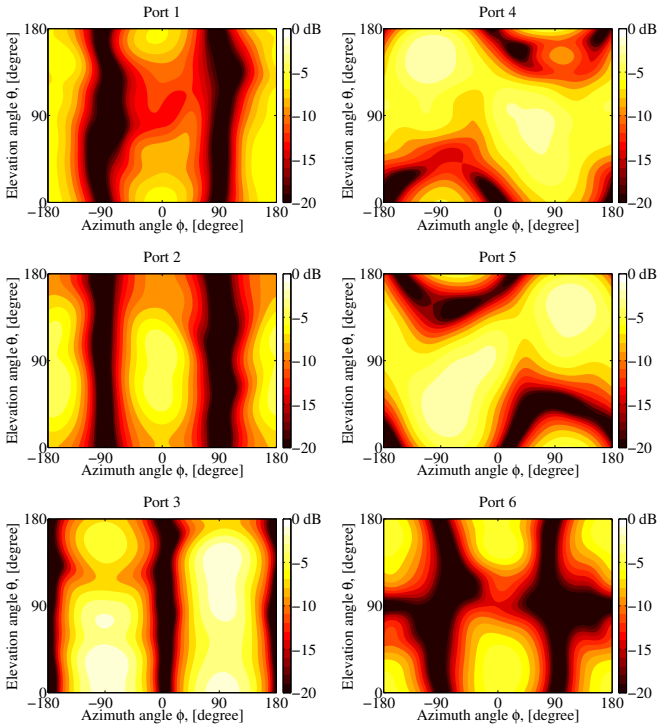

Fig. 4. Measured gain patterns of the reference TX array, $G_{\mathrm{TX},\phi}(\phi,\theta)$.

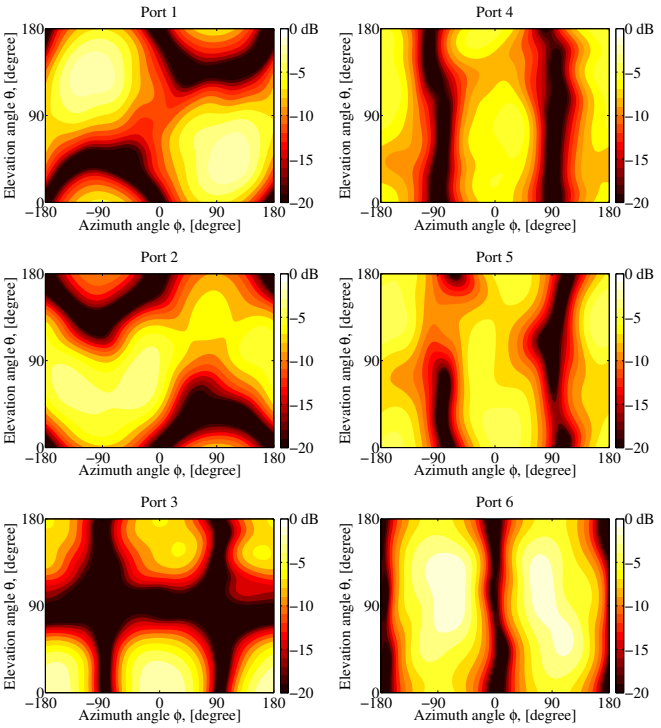

Fig. 5. Measured gain patterns of the reference TX array, $G_{\mathrm{TX},\theta}(\phi,\theta)$.

B. Compact RX Array

1) Array Design: In the RX array, smaller antennas are desired in order to co-locate the antenna elements. After studying dipoles with different lengths, a compromise is made between performance and size. Quarter-wave dipoles with the length of $200\,\mathrm{mm}$ can be matched to $50\,\Omega$ using a simple L-network. For the magnetic dipoles, electrically small planar split ring resonator (SRR) antennas [26] are considered. Figure 2(b) illustrates the design principle of the planar SRR antenna. Two circular loop wires with opposite openings are coupled fed by the inner circular dipole. The resonant frequency is mainly determined by the radius r. The impedance matching can be achieved by tuning the openings a, b and c. Single-sided PCB with a $1.55\,\mathrm{mm}$ thick FR4 substrate is used for the prototype. The width of the wires and the gaps between them are $2\,\mathrm{mm}$. Using CST, $r = 29.5\,\mathrm{mm}$, $a = b = 2\,\mathrm{mm}$ and $c = 19.6\,\mathrm{mm}$ are obtained for the center frequency of $377\,\mathrm{MHz}$.

Figure 1(b) shows the compact RX array. Three quarter-wave dipoles (Ports 1-3) are placed perpendicularly to one another and are essentially co-located at the center of the array structure. Three complementary magnetic dipoles (Ports 4-6) realized with the planar SRR antennas are also perpendicular to one another and are placed near one end of the quarter-wave dipoles in order to avoid strong mutual coupling. Consequently, the magnetic dipoles are about 0.1λ away from the array center. The maximum dimension of the array is determined by the quarter-wave dipoles, whose length can be reduced slightly in the presence of the SRR antennas, due to their proximity to the substrate material. As a result, the RX array can be enclosed in a small cubic volume of $(0.24\lambda)^3$. The compactness of the RX array is a substantial improvement in comparison to the existing compact arrays listed in Table I.

2) Array Characteristics: The measured S parameters are shown in Fig. 6. Due to the use of electrically compact

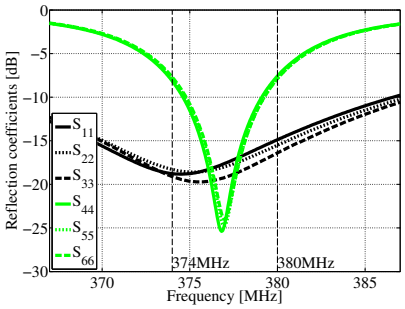

(a) Reflection coefficients: RX array

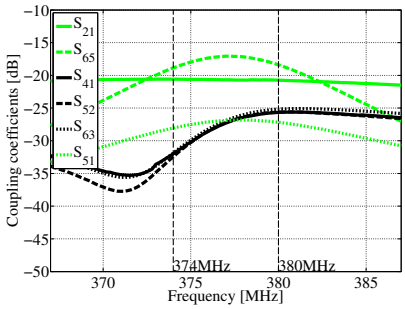

(b) Coupling coefficients: RX array

Fig. 6. Measured S parameters of the compact RX array. Ports 1-3 denote quarter-wave dipoles and Ports 4-6 denote SRR antennas, respectively.

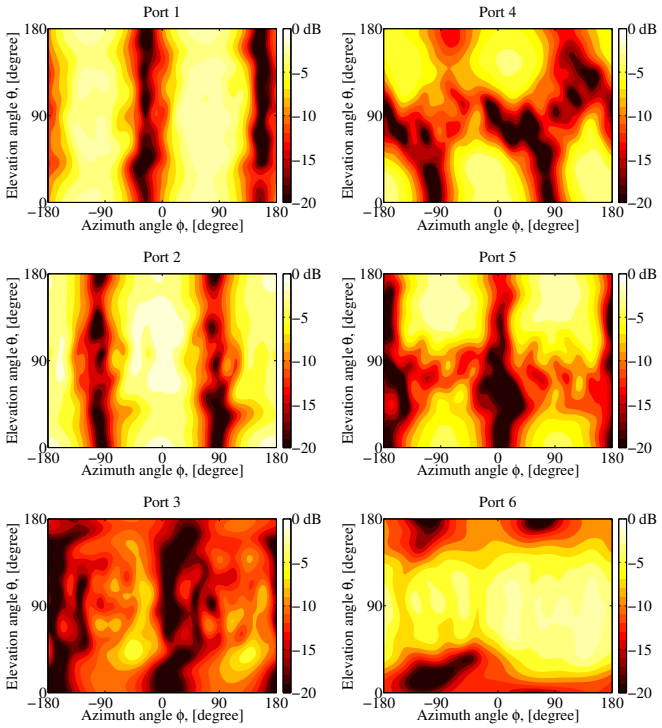

Fig. 7. Measured gain patterns of the compact RX array, $G_{\mathrm{RX},\phi}(\phi,\theta)$.

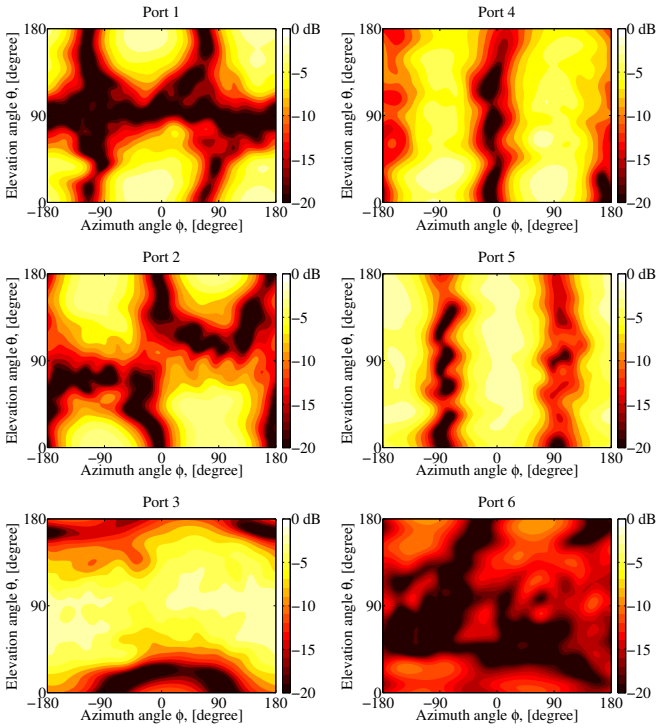

Fig. 8. Measured gain patterns of the compact RX array, $G_{\mathrm{RX},\theta}(\phi,\theta)$.

antennas, special attention is paid to the connecting RF coaxial cables. For this purpose, coaxial cables integrated with wide-band RF ferrite beads are used to minimize their influence on the antennas. The magnetic dipoles realized by the SRR antennas exhibit a much smaller bandwidth ($8\,\mathrm{MHz}$ at the $-6\,\mathrm{dB}$ level) relative to that of the electric dipoles. Due to the compactness, the isolation is slightly worse than the case of the TX array, especially between the loops. Nevertheless, a minimum isolation of $17\,\mathrm{dB}$ can still be achieved. It is noted that the design parameters as obtained from simulation are retuned for the fabricated prototypes, in order to maintain the center frequency of $377\,\mathrm{MHz}$. As a result, $a = 15\,\mathrm{mm}$, $b = 13\,\mathrm{mm}$ and $c = 32\,\mathrm{mm}$ for the prototypes.

For the radiation pattern measurements, a radio-over-fiber (ROF) system (see Fig. 9) is connected to the antenna under test, whereas the other five ports are terminated in $50\,\Omega$ loads. The ROF system is custom-developed to replace the RF cable for feeding the antenna, similar to that used in [27]. It consists of a laser diode (LD) module and a photo diode (PD) module. In passive measurements, the LD module is connected to the receiving antenna under test and it modulates the received RF signal into an optical signal. The PD module, connected to the LD module via an optical fiber, detects the RF signal from the optical signal and transfers it to the measurement equipment. The average total efficiency of the RX array is approximately $25\%(-6.0\,\mathrm{dB})$ for both the electric and magnetic dipoles. The relatively low efficiency can be explained by the use of lossy lumped elements in matching the quarter-wave dipoles, and the use of lossy FR4 substrate in making the SRR antennas. The measured gain patterns of the RX array in Figs. 7 and 8 are similar to those of the TX array, where good polarization and angle diversities can be observed.

The correlation between all pairs of the RX antenna radiation patterns is found to be less than 0.32, which is higher

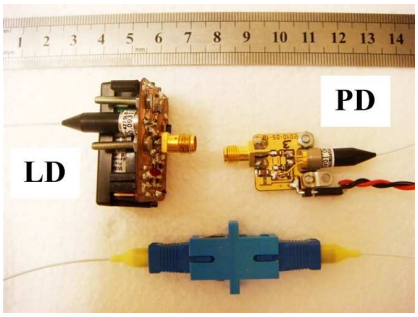

Fig. 9. Custom-developed ROF system with the LD and PD modules.

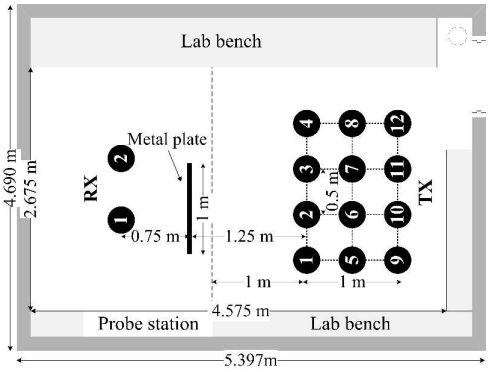

Fig. 10. Floor map of the lab and the setup in the measurement campaign.

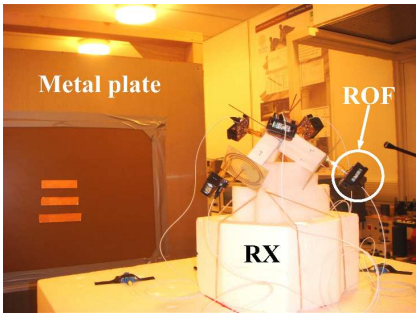

Fig. 11. The RX array with ROF systems in the MIMO channel measurement campaign. The metal plate was used to block the LOS path.

than that of the TX array. This is due to the compactness of the RX array. In practice, a complex correlation of below 0.7 in magnitude, or equivalently, an envelope correlation of below 0.5 is generally considered low enough to ensure good diversity gain and hence good DOF potential [9]. Nevertheless, an analysis on directly measured MIMO channels provides a more concise indication of the number of available DOFs.

Table II summarizes the characteristics of the two arrays.

III. Channel Measurement Campaign

In order to experimentally verify the number of DOFs in a real propagation channel, a MIMO channel measurement campaign was conducted in a RF shielded laboratory (see Fig. 10). This is because that the propagation environment inside the lab is inherently of rich multipath scattering, due to its inner metallic walls/ceiling/floor and the presence of lab equipments and office furniture at the time of the measurement (not all shown in Fig. 10). The dimensions of the lab are $5.40\,\mathrm{m}$ (length) $\times$ $4.69\,\mathrm{m}$ (width) $\times$ $2.51\,\mathrm{m}$ (height). It is noted here that one limitation of the experiment is that the measured environment is not very large with respect to the wavelength at $377\,\mathrm{MHz}$ ($\lambda \approx 0.8\,\mathrm{m}$). Therefore, the far-field condition is not ensured in the measurement setup, which means that the achieved results may not necessarily apply to typical indoor wireless systems such as IEEE802.11 standards that operate at $2.4/5\,\mathrm{GHz}$. In order to avoid any dominant propagation path, a big metal plate was used to block the Line-of-Sight (LOS) between the TX and RX arrays (shown in Fig. 10 for one RX position). Each antenna array was mounted on top of a trolley, at a height of $0.8\,\mathrm{m}$. Electrically neutral Rohacell foam units were used to support the array structures on the trolleys. Figure 11 shows the RX part of the measurement setup. During the measurements, the two trolleys were stationed at different measurement locations inside the lab, as labeled in Fig. 10. In total, two RX positions together with 12 TX positions were measured in order to obtain good fading statistics. Adjacent TX measurement positions were $0.5\,\mathrm{m}$ (*i.e.*, more than $\lambda/2$) apart from each other. In addition, 4 different orientations of 90° angular separation were utilized at each TX/RX position, which resulted in a total of 384 ($2 \times 4 \times 12 \times 4$) unique measurement runs.

TABLE II
Characteristics of the TX and RX six-port arrays.

	Size	Bandwidth ($-6\,\mathrm{dB}$)	Efficiency Dipole, Loop	Correlation $\max\|r_{ij}\|$
TX	$(0.75\lambda)^3$	$13.6\,\mathrm{MHz}(3.6\%)$	88.4%, 60.9%	0.13
RX	$(0.24\lambda)^3$	$8\,\mathrm{MHz}(2.1\%)$	25%, 25%	0.32

The 6×6 channel transfer functions between the TX/RX antennas were measured using the Medav RUSK Lund wideband channel sounder, enabled by fast RF switching. The channel sounder, which performs MIMO channel measurements based on the "switched array" principle [28], was stationed outside the lab. As shown in Fig. 11, the ROF systems were used for connecting each port of the compact RX array to the 6-to-1 switch. The measurements were performed using 65 subcarrier signals over a $20\,\mathrm{MHz}$ bandwidth centered at $377\,\mathrm{MHz}$. However, only the measured data over the center $6\,\mathrm{MHz}$ bandwidth were used for this study due to the limited bandwidth of the RX array, as can be seen in Fig. 6(a). This corresponds to 21 samples which are used as narrowband frequency channel realizations. A block of 400 consecutive snapshots was obtained for each measurement run (of a given TX/RX array position/orientation). To ensure that we actually measured the channel, rather than only the noise, the impulse responses were visually checked throughout the measurement campaign. The measured snapshots are used in post processing to estimate the noise variance [19]. The mean of all snapshots is taken as the measured channel for the given TX/RX array position/orientation. This is to enhance signal-to-noise ratio (SNR) of the measurement. As a result, the achieved post processing SNR is on average $30\,\mathrm{dB}$.

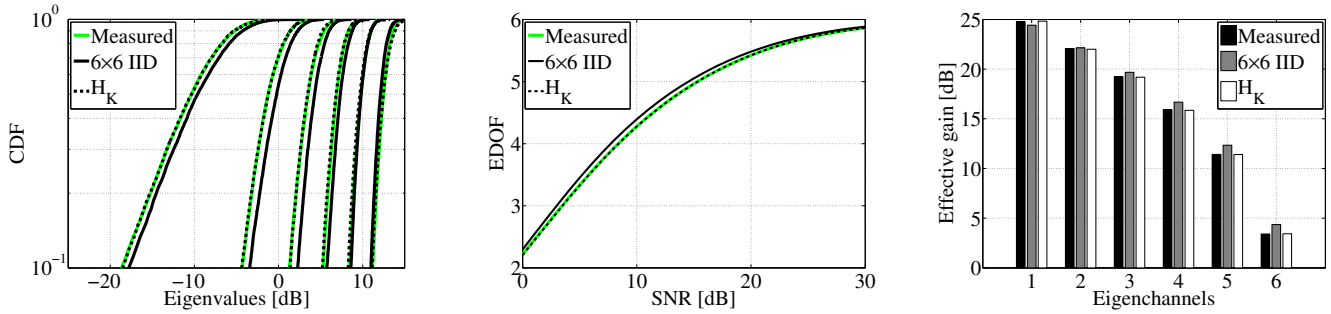

(a) Distribution of eigenvalues (b) EDOF (c) Effective eigenchannel gain

Fig. 12. Eigenvalue analysis of the measured MIMO channels in comparison to the 6×6 IID Rayleigh channels.

IV. Number of DOFs

It is known that the MIMO channel $\mathbf{H}$ can be decomposed into a subset of eigenchannels. With equal TX power allocation, the MIMO channel capacity is expressed as the sum of the capacities of all the eigenchannels [29], *i.e.*,

$$C = \sum_{k=1}^{\kappa} \log(1 + \frac{\rho}{M_{\mathrm{T}}} \alpha_k^2) = \sum_{k=1}^{\kappa} \log(1 + \gamma_k), \qquad (1)$$

where α_k^2 $(k = 1, 2, \ldots, \kappa)$ are the positive eigenvalues of $\mathbf{H}\mathbf{H}^H$ with the rank of $\mathbf{H}$ denoted by κ, ρ denotes the SNR. In turn, the effective power gain of each eigenchannel is determined by γ_k. In order to compare the measured eigenvalues to those of independent and identically distributed (IID) Rayleigh MIMO channels $\mathbf{H}_{\mathrm{w}}$, the measured channels are normalized according to *Method 1 - Normalized received SNR* in [19]. For the individual measurement run taken at a given TX/RX array position/orientation, the measured channel matrices are normalized over the frequency samples (or narrowband channel realizations) against a constant power term. In this way, the large scale fading among the 384 independent measurement runs is neglected. Meanwhile, the small scale fading of the narrowband channel realizations of each measurement, as well as the gain imbalance among the channel branches is preserved. The normalized channel matrices can then be used as data samples for obtaining relevant statistics of the results.

In Fig. 12(a), the cumulative distribution functions (CDFs) of the eigenvalues can be seen to closely follow those of the 6×6 IID Rayleigh channels. In order to quantify the number of eigenchannels that can be exploited for spatial multiplexing, the concept of effective DOF (EDOF) [30] is employed. The EDOF performance is illustrated in Fig. 12(b). With high enough SNR, six DOFs are clearly attained in the measured channels. Furthermore, the average effective power gain of each eigenchannel γ_k is shown in Fig. 12(c). The evaluation is performed with $20\,\mathrm{dB}$ SNR. This is $10\,\mathrm{dB}$ lower than the measurement SNR to ensure better accuracy and avoid overestimating the performance. With the simple equal TX power allocation, even the weakest eigenchannel can achieve a positive effective power gain, and the effective power gains of the measured and IID channels differ by at most $1\,\mathrm{dB}$.

The small degradation can be caused by either insufficient richness of the multipath propagation or imperfect MIMO antennas. As pointed out earlier, the measured non-LOS scenario inside the RF shielded lab is expected to be rich in multipath scattering. This is confirmed by the Rayleigh distributed measured channel envelopes. In particular, a Rician distribution with a negligibly small K-factor of 0.87 is obtained. On the other hand, it is evident from the measured array characteristics in Table II that the TX and RX arrays are imperfect. The correlation and efficiency imbalance between the antennas is known to result in performance degradation in the context of multiplexing efficiency [31]. To quantify their impacts on the DOF of a rich multipath (*i.e.*, IID Rayleigh) channel, we employ the Kronecker model [29] as defined by $\mathbf{H}_{\mathrm{K}} = \mathbf{R}_{\mathrm{RX}}^{1/2} \mathbf{H}_{\mathrm{w}} (\mathbf{R}_{\mathrm{TX}}^{1/2})^T$, where $\mathbf{R}_{\mathrm{RX}}$ and $\mathbf{R}_{\mathrm{TX}}$ denotes the correlation matrix of the RX and TX arrays, respectively. It is known that the Kronecker model will fail to predict the performance of a channel when there exists strong correlation between the respective local APS at the TX and RX ends [32]. However, the measured rich scattering environment is expected to facilitate separable APSs.

According to [31], the correlation matrix $\mathbf{R}$ (*i.e.*, $\mathbf{R}_{\mathrm{RX}}$ or $\mathbf{R}_{\mathrm{TX}}$) can fully characterize the correlation and efficiency imbalance among the antennas. It can be expressed as $\mathbf{R} = \mathbf{\Lambda}^{1/2} \bar{\mathbf{R}} \mathbf{\Lambda}^{1/2}$, where $\mathbf{\Lambda}$ is a diagonal matrix whose (i,i)th entry denotes the total efficiency of the ith antenna. $\bar{\mathbf{R}}$ is a normalized correlation matrix whose (i,j)th entry represents the correlation coefficient between the ith and jth antennas. In this way, $\mathbf{H}_{\mathrm{K}}$ is obtained by modifying $\mathbf{H}_{\mathrm{w}}$ according to the measured correlation and efficiency imbalance among the array elements at the RX and TX ends, respectively. In Figs. 12(a), 12(b) and 12(c), the eigenvalues obtained from $\mathbf{H}_{\mathrm{K}}$ are observed to be practically identical to those of the measured channels. Therefore, the Kronecker model which assumes separable TX/RX APSs is confirmed to be valid in this scenario. This observation also reveals that the small performance degradation obtained from the measurements can be mainly attributed to practical constraints in achieving perfect six-port antenna arrays. Despite the use of the compact RX array with co-located antennas, the results clearly show that six eigenchannels are attained, and they closely resemble those offered by the IID Rayleigh channels.

V. Conclusions

In this study, we have conducted an experiment using two six-port antenna arrays which are designed by means of

tri-polarized antenna pairs of electric and magnetic dipoles. Experimental results of the MIMO channel measurements performed in a RF shielded laboratory verify that six eigenchannels are attained. In particular, one array (RX) is made compact with all antenna elements enclosed in a small cubic volume of $(0.24\lambda)^3$. The three electric dipoles are co-located at the center of the array, whereas the magnetic dipoles are placed at about 0.1λ from the array center. The achieved compactness is a substantial improvement in comparison to existing implemented designs in the literature. In fact, the achieved size approaches the analytical limit obtained from [11], where the MIMO cube needs to be as large as $(0.2\lambda)^3$ in order to obtain six DOFs, if mutual coupling is taken into account.

Apart from the reported NLOS scenario, measurements have also been performed without the metal plate that blocks the LOS path. This is interesting because only two DOFs are theoretically available in the presence of a strong LOS component. However, as low Rician K-factors are still obtained, the scattering components are as significant as the LOS component inside the RF shielded lab. In addition, we verified that space diversity does not contribute significantly to the achieved DOFs in the compact array. This is done by examining the DOF performance of $\mathbf{H}_{\mathrm{K}}$ as synthesized from the measured array patterns and a simulated Gaussian APS with narrow angular spread at the RX end, assuming ideal conditions at the TX end ($\mathbf{R}_{\mathrm{TX}} = \mathbf{I}_6$). For the compact RX array, two effective DOFs are achieved in this scenario, whereas large arrays (such as the TX array in this paper) readily offer higher effective DOFs due to space diversity.

ACKNOWLEDGMENT

The authors would like to thank Thomas Bolin, Vanja Plicanic, Dmytro Pugachov and Zhinong Ying of Sony Ericsson Mobile Communications AB for their help with the antenna measurements, and Alessandro Scannavini of SATIMO for the calibration antenna. Kind support from Lars Hedenstjerna, Martin Nilsson and Ivaylo Vasilev are also acknowledged.

REFERENCES

[1] J. Winters, "On the capacity of radio communication systems with diversity in a Rayleigh fading environment," *IEEE J. Sel. Areas Commun.*, vol. 5, no. 5, pp. 871 – 878, Jun. 1987.

[2] W. Lee and Y. Yeh, "Polarization diversity system for mobile radio," *IEEE Trans. Commun.*, vol. 20, no. 5, pp. 912 – 923, Oct. 1972.

[3] R. Andrews, P. Mitra, and R. deCarvalho, "Tripling the capacity of wireless communications using electromagnetic polarization," *Nature*, vol. 409, pp. 316 – 318, Jan. 2001.

[4] A. Poon, R. Brodersen, and D. Tse, "Degrees of freedom in multiple-antenna channels: a signal space approach," *IEEE Trans. Inf. Theory*, vol. 51, no. 2, pp. 523 – 536, Feb. 2005.

[5] M. Migliore, "On the role of the number of degrees of freedom of the field in MIMO channels," *IEEE Trans. Antennas Propag.*, vol. 54, no. 2, pp. 620 – 628, Feb. 2006.

[6] M. Gustafsson and S. Nordebo, "Characterization of MIMO antennas using spherical vector waves," *IEEE Trans. Antennas Propag.*, vol. 54, no. 9, pp. 2679 – 2682, Sep. 2006.

[7] M. S. Elnaggar, S. K. Chaudhuri, and S. Safavi-Naeini, "Multi-polarization dimensionality of multi-antenna systems," *Progress In Electromagnetics Research B*, vol. 14, no. 2, pp. 45 – 63, 2009.

[8] T. Svantesson, M. Jensen, and J. Wallace, "Analysis of electromagnetic field polarizations in multiantenna systems," *IEEE Trans. Wireless Commun.*, vol. 3, no. 2, pp. 641 – 646, Mar. 2004.

[9] R. Vaughan and J. B. Andersen, *Channels, Propagation and Antennas for Mobile Communications*. London: The IEE, 2003.

[10] B. Getu and J. Andersen, "The MIMO cube - a compact MIMO antenna," *IEEE Trans. Wireless Commun.*, vol. 4, no. 3, pp. 1136 – 1141, May 2005.

[11] B. Getu and R. Janaswamy, "The effect of mutual coupling on the capacity of the MIMO cube," *IEEE Antennas Wireless Propag. Lett.*, vol. 4, pp. 240 – 244, 2005.

[12] D. Stancil, A. Berson, J. Van't Hof, R. Negi, S. Sheth, and P. Patel, "Doubling wireless channel capacity using co-polarised, co-located electric and magnetic dipoles," *Electron. Lett.*, vol. 38, no. 14, pp. 746 – 747, Jul. 2002.

[13] D. Skaufel, "Dual polarized omnidirectional antenna," Master's thesis, Royal Institute of Technology, KTH, Stockholm, Sweden, 2005.

[14] A. Alford and A. Kandoian, "Ultra-high frequency loop antennae," *Electrical Communication*, vol. 18, pp. 255 – 265, 1940.

[15] C. Y. Chiu, J. B. Yan, and R. Murch, "Compact three-port orthogonally polarized MIMO antennas," *IEEE Antennas Wireless Propag. Lett.*, vol. 6, pp. 619 – 622, Dec. 2007.

[16] G. Gupta, B. Hughes, and G. Lazzi, "On the degrees of freedom in linear array systems with tri-polarized antennas," *IEEE Trans. Wireless Commun.*, vol. 7, no. 7, pp. 2458 – 2462, Jul. 2008.

[17] A. Konanur, K. Gosalia, S. Krishnamurthy, B. Hughes, and G. Lazzi, "Increasing wireless channel capacity through MIMO systems employing co-located antennas," *IEEE Trans. Microw. Theory Tech.*, vol. 53, no. 6, pp. 1837 – 1844, Jun. 2005.

[18] C. Y. Chiu, J. B. Yan, R. Murch, J. Yun, and R. Vaughan, "Design and implementation of a compact 6-port antenna," *IEEE Antennas Wireless Propag. Lett.*, vol. 8, pp. 767 – 770, Dec. 2009.

[19] R. Tian, V. Plicanic, B. K. Lau, and Z. Ying, "A compact six-port dielectric resonator antenna array: MIMO channel measurements and performance analysis," *IEEE Trans. Antennas Propag.*, vol. 58, no. 4, pp. 1369 – 1379, Apr. 2010.

[20] C. Y. Chiu, J. B. Yan, and R. Murch, "24-port and 36-port antenna cubes suitable for MIMO wireless communications," *IEEE Trans. Antennas Propag.*, vol. 56, no. 4, pp. 1170 – 1176, Apr. 2008.

[21] I. Kovalyov and D. Ponomarev, "Small-size 6-port antenna for three-dimensional multipath wireless channels," *IEEE Trans. Antennas Propag.*, vol. 54, no. 12, pp. 3746 – 3754, Dec. 2006.

[22] L. Lo Monte, B. Elnour, D. Erricolo, and A. Nehorai, "Design and realization of a distributed vector sensor for polarization diversity applications," in *Proc. Int. Waveform Diversity and Design Conf.*, Pisa, Italy, 4-8 Jun. 2007, pp. 358 – 361.

[23] J. Tabrikian, R. Shavit, and D. Rahamim, "An efficient vector sensor configuration for source localization," *IEEE Signal Process. Lett.*, vol. 11, no. 8, pp. 690 – 693, Aug. 2004.

[24] "CST Homepage," *http://www.cst.com*.

[25] "SATIMO Homepage," *http://www.satimo.fr*.

[26] O. Kim, "Low-Q electrically small spherical magnetic dipole antennas," *IEEE Trans. Antennas Propag.*, vol. 58, no. 7, pp. 2210 – 2217, Jul. 2010.

[27] S. Kurokawa and M. Hirose, "A new balun for antenna measurement using photonic sensor," in *Proc. 2nd Eur. Conf. Antennas Propag. (EuCAP 2007)*, Edinburgh, UK, 11 - 16 Nov. 2007.

[28] R. Thoma, D. Hampicke, A. Richter, G. Sommerkorn, A. Schneider, U. Trautwein, and W. Wirnitzer, "Identification of time-variant directional mobile radio channels," *IEEE Trans. Instrum. Meas.*, vol. 49, no. 2, pp. 357 – 364, Apr. 2000.

[29] A. Paulraj, R. Nabar, and D. Gore, *Introduction to Space-Time Wireless Communications*. New York: Cambridge University Press, 2003.

[30] D.-S. Shiu, G. Foschini, M. Gans, and J. Kahn, "Fading correlation and its effect on the capacity of multielement antenna systems," *IEEE Trans. Commun.*, vol. 48, pp. 502 – 513, Mar. 2000.

[31] R. Tian, B. K. Lau, and Z. Ying, "Multiplexing efficiency of MIMO antennas," *IEEE Antennas Wireless Propag. Lett.*, vol. 10, pp. 183 – 186, 2011.

[32] H. Özcelik, M. Herdin, W. Weichselberger, J. Wallace, and E. Bonek, "Deficiencies of the Kronecker MIMO radio channel model," *Electron. Lett.*, vol. 39, pp. 1209 - 1210, Aug. 2003.

Ruiyuan Tian (S'07) received the Ph.D. degree from the engineering faculty of Lund University (LTH), Sweden, in 2011, the M.Sc. degree from Chalmers University of Technology (CTH), Sweden, in 2007, and the Bachelor's degree from Beijing Institute of Technology (BIT), China, in 2005, all in electrical engineering with focus on radio communications.

During 2007 and 2011, he conducted research in design and evaluation of compact multi-antennas for efficient MIMO communications. During 2006 to 2007, he worked as a guest researcher in the Telecommunications Research Center in Vienna (FTW), Austria. In the meantime, he also finished his master's thesis on clustering and tracking in MIMO radio channel modeling. In 2005, he carried out field measurements and analysis in his bachelor's degree project using a test-bed based on WLAN ad-hoc networks.

Dr. Tian's current research interests include antenna systems, propagation channels, as well as signal processing topics in wireless communications.

Buon Kiong Lau (S'00M'03SM'07) received the B.E. degree (with honors) from the University of Western Australia, Perth, Australia and the Ph.D. degree from Curtin University of Technology, Perth, in 1998 and 2003, respectively, both in electrical engineering.

During 2000 to 2001, he worked as a Research Engineer with Ericsson Research, Kista, Sweden. From 2003 to 2004, he was a Guest Research Fellow at the Department of Signal Processing, Blekinge Institute of Technology, Sweden. Since 2004, he has been at the Department of Electrical and Information Technology, Lund University, where he is now an Associate Professor. He has been a Visiting Researcher at the Department of Applied Mathematics, Hong Kong Polytechnic University, China, Laboratory for Information and Decision Systems, Massachusetts Institute of Technology, and Takada Laboratory, Tokyo Institute of Technology, Japan. His primary research interests are in various aspects of multiple antenna systems, particularly the interplay between antennas, propagation channels and signal processing.

Dr. Lau is an Associate Editor for the IEEE TRANSACTIONS ON ANTENNAS AND PROPAGATION and a Guest Editor of the 2012 Special Issue on MIMO Technology for the same journal. From 2007 to 2010, he was a Co-Chair of Subworking Group 2.2 on "Compact Antenna Systems for Terminals" (CAST) within EU COST Action 2100. Since 2011, he is a Swedish national delegate and the Chair of Subworking Group 1.1 on "Antenna System Aspects" within COST IC1004.